PAPER

Check for updates

Subtle chemical modification for enrichment of Fmoc-amino acid at a phospholipid interface†

Pablo G. Argudo, [a] Rafael Contreras-Montoya,[b] Luis Álvarez de Cienfuegos, *[b] María T. Martín-Romero, [a] Luis Camacho [a] and Juan J. Giner-Casares *[a]

Amino acids including the Fmoc group (9-fluorenylmethyloxycarbonyl) are bioinspired molecules that display intriguing features in self-assembly and biological applications. The influence of a delicate chemical modification between Fmoc-F and Fmoc-Y on the interaction with a phospholipid surface was analyzed. Langmuir monolayers of the 1,2-dimyristoyl-*sn-glycero*-3-phosphate (DMPA) phospholipid were used to mimic the eukaryotic cell membrane. *In situ* Brewster angle microscopy and UV-vis reflection spectroscopy provided insights on the effect of the Fmoc-amino acid derivatives on the DMPA phospholipid. The formation of H-bonds between the Fmoc-Y and the DMPA molecules was assessed, demonstrating the crucial role of the hydroxyl group of Fmoc-Y in enhancing the interaction with biosurfaces.

Introduction

Fmoc-amino acids are highly valuable elements in nanoscience as recently shown by Yan *et al.*, demonstrating co-assembly of Fmoc-His with phthalocyanine into nanovesicles as catalysts.[1] Fmoc-amino acids are excellent hydrogelators as well.[2–4] Fmoc-amino acids have been successfully included in nanocomposite structures for drug delivery.[5,6] Additional biological applications of the Fmoc-amino acids include their use as effective antibacterial agents.[7] The versatility of Fmoc-amino acids for combining with other inorganic and organic nanoparticles led to interesting hybrid materials including graphene oxide.[8] Partition coefficient (*P*) was proven a key parameter for Fmoc-dipeptides in interfacial self-assembly and interaction with lipid monolayers.[9,10] The surface activity of the Fmoc-amino acids played a significant role in the capability for self-assembly.[11] The hydrophobicity of the Fmoc-Met has been related with the formation of amyloid fibrils.[12] Gazit *et al.* reported on the complementary self-assembly of amino acids for tuning the intermolecular interactions, confirming the hypothesis that slight chemical modifications might have a large impact in the obtained supramolecular structures.[13]

Motivated by the relevance of the Fmoc-amino acids in biological applications, the interaction of two related Fmoc-amino

acids with a model eukaryotic cell membrane has been explored. A Langmuir monolayer of the 1,2-dimyristoyl-*sn-glycero*-3-phosphate (DMPA) phospholipid provided a convenient model for the eukaryotic cell surface. The Langmuir technique allows a fine adjustment of the area per phospholipid molecule. Experimental *in situ* characterization of the effect of the Fmoc-amino acids on the phospholipid monolayer was performed.[14,15] Brewster Angle Microscopy (BAM) was used to examine the morphology of the phospholipid monolayer, attaining relevant information on the lipid domains.[16,17] UV-vis reflection spectroscopy allowed to monitor the presence of the Fmoc-amino acids at the phospholipid interface by the characteristic UV-vis signal from the Fmoc group.[18,19] We also examined the specific intermolecular interactions of DMPA with the Fmoc-amino acids and found that Fmoc-Y showed superior performance when interacting with the phospholipid surface by molecular mechanics computational simulations.[20]

Results and discussion

A Langmuir monolayer of the DMPA phospholipid was used as model for the eukaryotic cell surface, see Fig. 1 for the molecular structures. Two Fmoc-amino acid derivatives were studied, Fmoc-F and Fmoc-Y. Both Fmoc-amino acid derivatives share the same molecular structure, with an additional hydroxyl terminal group for the latter, see Fig. 1. The Fmoc-amino acid derivatives are highly soluble in water. We followed the strategy described by Adams and Clegg to enhance the residence of the Fmoc-amino acid derivatives at the air/water interface, using pH = 2 of the subphase for avoiding the complete solving of the Fmoc-amino acids spread at the air/water interface.[21] The Fmoc-amino acid derivatives were expected to be fully protonated at

[a]Departamento de Química Física y T. Aplicada, Instituto Universitario de Investigación en Química Fina y Nanoquímica IUNAN, Facultad de Ciencias, Universidad de Córdoba (UCO), Campus de Rabanales, Ed. Marie Curie, E-14071 Córdoba, Spain. E-mail: jjginer@uco.es

[b]Departamento de Química Orgánica, Facultad de Ciencias, Universidad de Granada, (UGR), C. U. Fuentenueva, E-18071 Granada, Spain. E-mail: lac@ugr.es
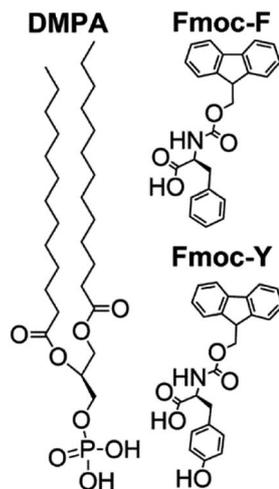
Fig. 1 Molecular structure of the 1,2-dimyristoyl-*sn-glycero*-3-phosphate (DMPA) phospholipid, Fmoc-phenylalanine (Fmoc-F) and Fmoc-tyrosine (Fmoc-Y).

Fig. 2 Surface pressure–molecular area isotherms for the DMPA : Fmoc-F mixed monolayer (red line), DMPA : Fmoc-Y mixed monolayer (blue line),and pure DMPA monolayer (black line).

this value of pH.[22,23] This study aims at providing a detailed description of the molecular interactions between the Fmoc-amino acid derivatives and the DMPA phospholipid monolayer as a simplified model of the highly complex surface of a eukaryotic cell membrane. Note that phosphatidylcholine (PC) lipids constitute the largest fraction of phospholipids in a eukaryotic cell membrane, with no net charge at physiological pH. However, a pH = 2 subphase is required as commented above, resulting in net positive charge of the polar head group of PC lipids. Therefore PC lipids were replaced by DMPA herein. DMPA phospholipid is protonated at pH = 2, displaying no net charge and being therefore closer to the biological scenario than the PC lipids.[24]

We note that the DMPA monolayer is not resembling to the actual and complex biological scenario. However, under the specified experimental conditions, the DMPA monolayer appears as the best compromise solution for a phospholipid surface that allows the study of the interactions with the Fmoc-amino acid derivatives. The mechanism of interaction between the Fmoc-amino acid and phospholipid molecules should not be greatly affected by the value of pH of the subphase.

Herein mixed monolayers of DMPA : Fmoc-amino acid 1 : 1 molar ratio, *i.e.*, equal number of molecules spread at the air/water interface, have been prepared. The surface pressure–molecular area isotherms for the mixed monolayers DMPA : Fmoc-F and DMPA : Fmoc-Y are shown in Fig. 2. The relative amount of Fmoc-amino acid derivative molecules with respect to the DMPA phospholipid molecules should allow the effective interaction at the mixed Langmuir monolayer, while preventing the excess of Fmoc-amino acid leading to self-aggregation and formation of pure Fmoc-amino acid macroscopic regions. Therefore, a molar ratio 1 : 1 was chosen according to previous reports in mixed monolayers including a DMPA lipid matrix.[25,26] An expansion of the isotherms for both DMPA : Fmoc-F and DMPA : Fmoc-Y monolayers comparing to the pure DMPA isotherm was observed. However, the expansion of the isotherm
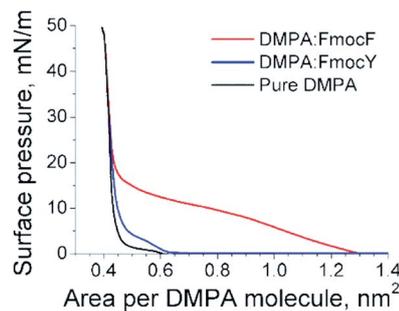
was significantly higher for Fmoc-F than for Fmoc-Y. This observation pointed to a comparatively reduced occupancy of the Fmoc-Y molecules at the DMPA monolayer. The difference between the isotherms for DMPA : Fmoc-F and DMPA : Fmoc-Y was more noticeable at low values of surface pressure, corresponding to an expanded state of the monolayer. The lift-off of the surface pressure took place at *ca.* 1.3 nm^2 per DMPA molecule for the DMPA : Fmoc-F monolayer, whereas surface pressure remains zero until *ca.* 0.7 nm^2 per DMPA molecule was reached in the DMPA : Fmoc-Y monolayer. The expansion of the DMPA : Fmoc-F with respect to the DMPA : Fmoc-Y isotherm from 0 to 5 mN m^{-1} was *ca.* 0.6 nm^2 per DMPA molecule. Assuming a surface area of 0.21 nm^2 per Fmoc-F molecule, the expansion in this region of the isotherm indicated an approximate number of three Fmoc-F molecules at the monolayer per molecule of DMPA. This is an approximation exclusively based on the surface area per Fmoc-F molecule assuming a completely upright arrangement. Miscibility experiments using mixed Langmuir monolayers of DMPA : Fmoc-F in different molar ratios would be relevant to attain insights on the molar ratio at the interface. Unfortunately, the significant tendency of the Fmoc-F molecules to be transferred to the bulk subphase with compression of the monolayer hindered the consistency of such experiment.[27] Thus, Fmoc-F showed a greater tendency to accommodate in an expanded monolayer, probably interacting *via* hydrophobic interactions between the Fmoc groups with the alkyl chains of the DMPA molecules. Note that these interactions were not able to sustain the Fmoc-F molecules when the mixed monolayer was subjected to compression. Instead, a constant loss of the Fmoc-F molecules to the bulk subphase was obtained, as demonstrated below by UV-vis reflection spectroscopy.

A region of reduced increase of surface pressure with compression of the monolayer similar to a plateau was observed from *ca.* 0.9 to 0.6 nm^2 per DMPA molecule for the DMPA : Fmoc-F mixed monolayer. This region might be connected with the liquid expanded-liquid condensed (LE-LC) transition and the transfer of Fmoc-F molecules from the mixed monolayer to the bulk subphase. Although the effect of these two processes could not be distinguished exclusively from the isotherm, the UV-vis reflection spectra informed on a significant transfer of

Fmoc-F to the bulk subphase, continuing the trend observed before. The isotherm for DMPA : Fmoc-Y showed a modest expansion and a similar shape to the isotherm for pure DMPA. This expansion was almost constant up to 10 mN m^{-1} and reached a value of *ca.* 0.03 nm^2 per DMPA molecule, *i.e.*, less than one Fmoc-Y molecule per twelve DMPA molecules. However, according to the UV-vis reflection spectra, the amount of Fmoc-amino acid was equal for both DMPA : Fmoc-F and DMPA : Fmoc-Y monolayers at *ca.* 0.7 nm^2 per DMPA molecule. Therefore, the Fmoc-Y molecules were adsorbed to the DMPA monolayer, residing at the phospholipid interface but occupying no space in the phospholipid region.

For both DMPA : Fmoc-F and DMPA : Fmoc-Y mixed monolayers a convergence with the isotherm for the pure DMPA at *ca.* 25 mN m^{-1} was obtained. This overlapping between the three isotherms indicated that both Fmoc-amino acids did not penetrate into the phospholipid monolayer at 30 mN m^{-1}. The phospholipid monolayer is equivalent to a bilayer at a surface pressure of 30 mN m^{-1}.[28,29] From purely thermodynamical arguments, the absence of any variation in the surface pressure–molecular area isotherm at 30 mN m^{-1} indicated no disruption of the phospholipid layer, thus pointing to a high biocompatibility concerning the rupture and modification of the cell surface.

The Fmoc-amino acids are soluble in water, showing a great tendency to form micelle-like aggregates. The Fmoc-amino acids can be solved in water up to 0.4 M, according to Pola-varapu *et al.*[11] Assuming a complete loss of the spread Fmoc-amino acid molecules from the air/liquid interface to the bulk subphase, a maximum concentration of 10^{-7} M would be achieved. Therefore, no influence of the solubility values of the Fmoc-F and Fmoc-Y was expected.

Brewster Angle Microscopy (BAM) provided direct visualization of the DMPA : Fmoc-amino acid mixed monolayers at the air/liquid interface, see Fig. 3.[30,31] Bright domains of LC phase appeared already at 0.8 nm^2 per DMPA molecule, with remarkable monodispersity in size and shape. The bright domains increased their size with compression of the DMPA monolayer up to *ca.* 10 mN m^{-1}. The domains coalesced into a homogenous solid phase for highly compressed state.[32] The morphology of the DMPA : Fmoc-F mixed monolayer was similar, with small and highly reflective dots appeared at 16 mN m^{-1}. Such bright dots were persistent and remained for the complete isotherm, and might be formed by a mixture of aggregated DMPA lipid molecules and a small fraction of Fmoc-F molecules.[33,34] Given the almost zero UV-vis reflection signal obtained for the DMPA : Fmoc-F mixed monolayer at 30 mN m^{-1} and the complete overlap of the isotherm with that of pure DMPA, the amount of Fmoc-F molecules was assumed to be close to zero. Thus, the bright dots might correspond to small aggregates of phospholipid formed by nucleation with the Fmoc-F molecules promoted by the hydrophobic interactions of the alkyl chains with the Fmoc group.

On the other hand, a significant modification of the morphology of the lipid domains was obtained for the DMPA : Fmoc-Y monolayer, probably caused by the interaction of the Fmoc-Y molecules with the polar head groups of the
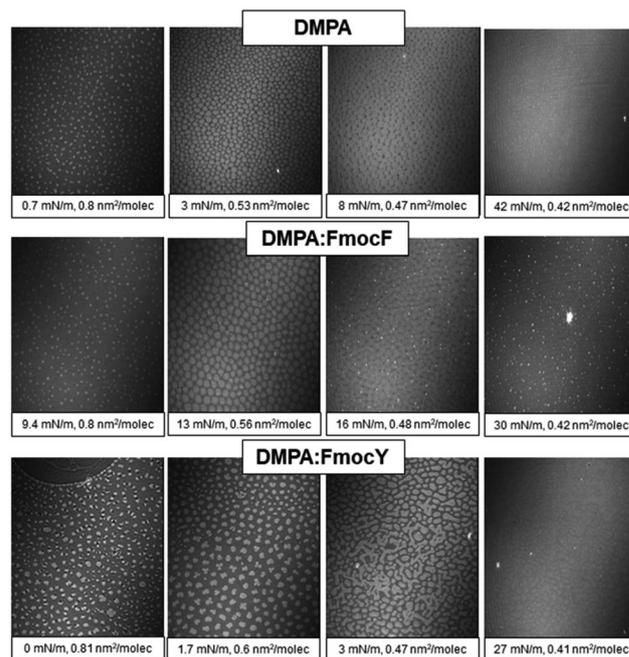

Fig. 3 Brewster angle microscopy images for the DMPA (top), DMPA : Fmoc-F (middle) and DMPA : Fmoc-Y (bottom) monolayers. The values of surface pressure and available surface area per DMPA molecule are included at the bottom of each picture. The width of each frame corresponds to 215 μm.

DMPA phospholipid that modified the line tension–electrostatic repulsion balance.[35] Not discrete but polydisperse domains that were connected to each other were obtained from 3 mN m^{-1} to further compressed state of the monolayer. A highly reflective and almost homogeneous morphology was obtained for the solid state of the monolayer, with no complete coalescence. An almost homogenous monolayer was obtained after compression of the monolayer to high values of surface pressure, indicating the expulsion of the Fmoc-Y molecules from the lipid monolayer to the adsorption region underneath the phospholipid head groups as confirmed by UV-vis reflection spectroscopy.

The presence of Fmoc-amino acid molecules in contact with the DMPA phospholipid monolayer was verified by UV-vis reflection spectroscopy, see Fig. 4. Note the UV-vis reflection signal for the pure DMPA monolayer was not significant along the complete isotherm of the DMPA. A small increase of the UV-vis reflection signal was found at the most compressed state of the DMPA monolayer, *i.e.*, 0.4 nm^2 per DMPA molecule. The UV-vis reflection signal was increased to a maximum value of 0.02 from 240 to 280 nm. On the other hand, the UV-vis reflection signal for the DMPA : Fmoc-Y mixed monolayer displayed a maximum intensity of *ca.* 0.09, showing a broad band from 240 to *ca.* 360 nm. Therefore, the contribution of the increase of reflection signal induced by the DMPA molecules was considered not significant for the UV-vis reflection spectra of the DMPA : Fmoc-F and DMPA : Fmoc-Y monolayers.

The bulk spectrum of Fmoc-F in bulk solution was formed by five components at 257, 266, 276, 290 and 300 nm, with the
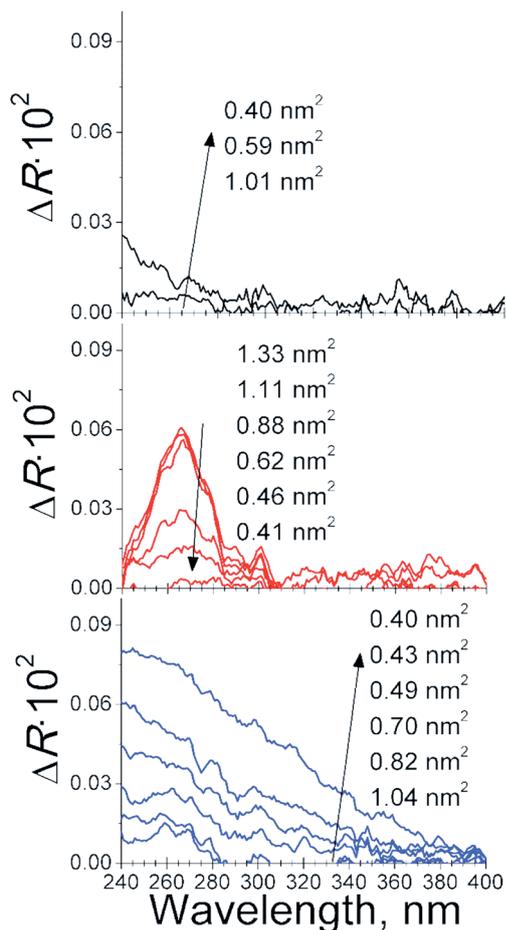
Fig. 4 UV-vis reflection for the pure DMPA (top, black line), DMPA : Fmoc-F (middle, red line) and DMPA : Fmoc-Y (bottom, blue line) monolayers. The values of available surface area per DMPA molecule are indicated in the inset.

most intense component at 266 nm, see Fig. S1.† The UV-vis reflection spectra of the DMPA : Fmoc-F mixed monolayer were formed by five components at 257, 266, 276, 290 and 301 nm, with the most intense component at 266 nm. The aggregation of the Fmoc-F molecules in contact with the DMPA molecules was therefore not significant. This finding was in agreement with the proposed model of the absence of a specific interaction between DMPA and Fmoc-F molecule at the air/liquid interface. The bulk spectrum of Fmoc-Y in bulk solution was formed by five components at 256, 266, 277, 290 and 300 nm, with the most intense component at 266 nm, see Fig. S1.† However, the UV-vis reflection spectra appeared as a broad band with no defined peaks from 240 to ca. 360 nm in the case of the DMPA : Fmoc-Y mixed monolayer, indicating a significant aggregation of the Fmoc-Y molecules. Note the intensity of the UV-vis reflection band displayed an intensity value more than four-fold higher than that of the pure DMPA monolayer at the most compressed state.

A significant amount of Fmoc-F molecules was already present at the expanded state of the DMPA : Fmoc-F mixed monolayer. The initial compression of the monolayer already decreased the surface concentration of Fmoc-F despite the significant expansion of the isotherm, as discussed above. The UV-vis reflection spectra for the DMPA : Fmoc-F mixed monolayer are similar to those found for the pure Langmuir assemblies of Fmoc-dipeptides at the air/water interface, thus pointing to a an upright conformation.[9] A change in the relative orientation of the Fmoc-F molecules at early stages of compression of the DMPA : Fmoc-F mixed monolayer might contribute to the overshoot in the surface pressure at 1.3 nm^2 per DMPA molecule with a modest decrease in the UV-vis reflection spectra to 0.9 nm^2 per DMPA molecule.

A significant loss of Fmoc-F molecules was observed with further compression from ca. 0.9 to 0.5 nm^2 per DMPA molecule, concurrent with the plateau observed in the isotherm. Thus, the expulsion of the Fmoc-F molecules from the mixed monolayer also contributed to the observed plateau in the isotherm, see Fig. 2. Remarkably, the Fmoc-F molecules were almost completely expelled from the air/liquid interface to the bulk subphase at the complete compression of the monolayer, with no UV-vis reflection signal obtained, see Fig. 5.

The DMPA : Fmoc-Y mixed monolayer displayed an opposite behavior to the DMPA : Fmoc-F monolayer. While no significant presence of the Fmoc-Y molecules was observed for the highly expanded state of the mixed monolayer, a steady enrichment of the Fmoc-Y molecules at the mixed monolayer with compression of the monolayer from ca. 0.8 nm^2 per DMPA molecule was obtained. The slight modification of the surface pressure–molecular area isotherm of the DMPA : Fmoc-Y mixed monolayer with respect to the isotherm of pure DMPA for low values of surface pressure and the complete overlap of both isotherms for values of surface pressure higher than 20 mN m^{-1} indicated the adsorption of Fmoc-Y molecules underneath the DMPA lipid monolayer.

Given that the Fmoc group was the source of the UV-vis reflection signal, the amount of the Fmoc-Y and Fmoc-F molecules at the mixed monolayer could be directly compared.[36] An intercrossing in the integral value of the UV-vis reflection
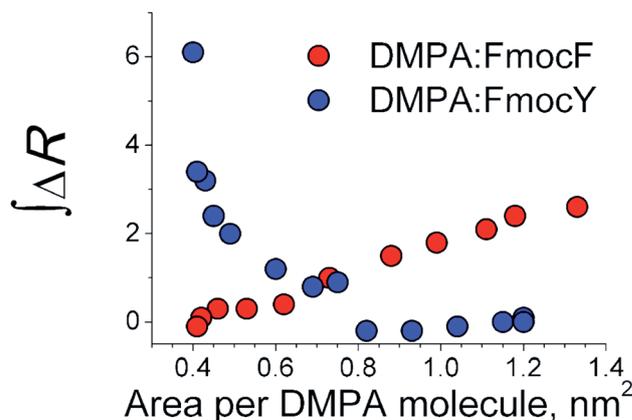

Fig. 5 Integral values of the UV-vis spectra for the DMPA : Fmoc amino acid derivatives at different values of available surface area per DMPA molecule. Composition of the mixed monolayers as noted in the inset.
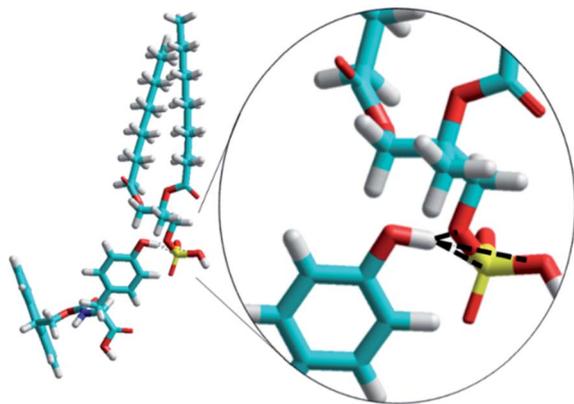
Fig. 6 Snapshot of the simulation of the DMPA : Fmoc–Y mixed monolayer. The intermolecular H–bonds are displayed as dashed black lines. Key color for atom type: light blue (carbon), red (oxygen) yellow (phosphorus) and deep blue (nitrogen).

spectra for the DMPA : Fmoc-F and DMPA : Fmoc-Y monolayers was found at *ca.* 0.7 nm^2 per DMPA molecule. The intercrossing was coincident with the plateau in the isotherm of the DMPA : Fmoc-F monolayer and values of surface pressure of 11 and 0 mN m^{-1} for the DMPA : Fmoc-F and DMPA : Fmoc-Y monolayers, respectively. Remarkably, the enrichment of Fmoc-Y with compression of the mixed monolayer led to a final surface concentration of Fmoc-Y being *ca.* two-fold higher than the initial surface concentration of Fmoc-F prior to compression of the monolayer, suggesting a superior capability of Fmoc-Y in interacting with the DMPA monolayer. Although the Fmoc-Y molecules did not occupy the phospholipid region, the interaction with the DMPA monolayer was more efficient than that of Fmoc-F, as noted by the significant enrichment in Fmoc-Y molecules. The location of the Fmoc-Y molecules underneath the DMPA monolayer might be the origin of the broadening and noise in the UV-vis reflection spectra, see Fig. 4. The aggregation of the Fmoc-Y molecules and a distribution of values of tilting angle of the Fmoc-Y molecules at the DMPA : Fmoc-Y mixed monolayer might also contribute to the broadening of the UV-vis peaks.

An opposite trend was found for the DMPA : Fmoc-F mixed monolayers. While Fmoc-F molecules showed a higher occupancy at the monolayer at the expanded state, the Fmoc-Y molecules were not present at such state, as evidenced by the shift in the surface pressure–molecular area isotherms and confirmed by the UV-vis reflection spectra. Hydrophobic interactions between the Fmoc group and the alkyl chains of the DMPA molecules might be responsible for this effect at the expanded state of the monolayer. A striking inversion of the effect of the Fmoc-amino acid molecules in the DMPA monolayer was observed with compression of the mixed monolayers. While the Fmoc-F molecules were gradually detached from the mixed monolayer, an enrichment of the mixed monolayer with Fmoc-Y molecules was detected. The intercrossing in the amount of Fmoc-amino acid took place during the plateau in the DMPA : Fmoc-F monolayer, with this region probably displaying simultaneously the phase transition of the

phospholipid and the expelling of the Fmoc-F molecules. This observation was consistent with the modification of the shape of the DMPA domains observed by BAM. Further compression of the mixed monolayers led to a complete removal of the Fmoc-F molecules from the mixed monolayers with no significant amount of Fmoc-F molecules adsorbed to the DMPA monolayer, as evidenced by the UV-vis reflection spectra. In contrast, the amount of Fmoc-Y molecules present at the phospholipid interface increased steadily to a maximum value at the highest value of surface pressure that was two-fold higher than the amount of the Fmoc-F molecules. Note the Fmoc-Y molecules were adsorbed underneath the DMPA monolayer, as confirmed by the overlap of the surface pressure–molecular area isotherms for DMPA, DMPA : Fmoc-F and DMPA : Fmoc-Y.

As commented above, we have used pH = 2 in the subphase to promote the residence of both Fmoc-F and Fmoc-Y. However, such experimental condition could not assure completely the presence of both Fmoc-amino acid derivatives at the air/water interface at all compression state of the DMPA monolayer. Instead, the residence of the Fmoc-amino acid derivatives at the mixed monolayers showed a great dependency on the compression state and the interactions with the DMPA phospholipid molecules.

The Fmoc-F molecule is slightly more hydrophobic than the Fmoc-Y molecules, with values of −log *P* of 4.7 and 4.4, respectively. This minor difference in hydrophobicity could not account for the radically different behavior of Fmoc-F and Fmoc-Y. To gain further insights into the specific intermolecular interactions between Fmoc-Y and DMPA, the formation of a complex was studied in more depth. Formation of H-bonds formed between the terminal hydroxyl group of Fmoc-Y and the polar head group of DMPA was expected. Molecular mechanics computational simulations were performed to examine the feasibility of the formation of H-bonds between the DMPA and Fmoc-Y molecules.[37,38] Three H-bonds were detected using *in vacuo* simulations, see Fig. 6. Note that using effective medium or including explicit water molecules could improve the simulations, as the effect of solvent would be taken into account. The terminal hydroxyl group of a single molecule of Fmoc-Y was able to form up to three H-bonds with a DMPA molecule. Two of the H-bonds were formed with the oxygen atoms from the phosphate group of the DMPA. Remarkably, the hydroxyl group of Fmoc-Y could also form a H-bond with the phosphorous atom from the phosphate group of DMPA, as recently described by Kjaergaard *et al.*[39]

Conclusions

The interactions between Fmoc-F and Fmoc-Y with a DMPA Langmuir monolayer as model eukaryotic cell surface were analyzed. Despite the hydroxyl group at the Fmoc-Y molecule as the unique chemical difference to Fmoc-F, an opposite behavior between the two Fmoc-amino acids was found. While Fmoc-F was present in the DMPA monolayer at the expanded state and was expelled with compression, Fmoc-Y was not in contact with the DMPA monolayer at the expanded state. A significant enrichment of the phospholipid interface with Fmoc-Y

molecules was demonstrated by UV-vis reflection spectroscopy. At the biologically relevant surface pressure of 30 mN m^{-1}, Fmoc-Y was found in higher surface concentration, indicating the superior interaction of Fmoc-Y with the phospholipid surface in contrast to the more hydrophobic Fmoc-F that was completely expelled to the bulk subphase. The origin of this enhanced interaction was the H-bonds formed by the hydroxyl group of Fmoc-Y with the phosphate group of DMPA. Therefore, purely thermodynamical considerations as given by the partition coefficient did not account for the experimental behavior of the Fmoc-amino acid derivatives. The subtle chemical modification of including a single hydroxyl group in the terminal side of the Fmoc-amino acid derivative could promote specific intermolecular interactions between the Fmoc-Y and the phospholipid surface, in this case H-bonds. Infrared reflection spectroscopy and neutron reflectivity measurements would be highly informative as well in detailing these interactions. This work suggest that the inclusion of hydroxyl groups that are capable of forming directed H-bonds is a straightforward strategy to improve the biological application of assemblies based on Fmoc-amino acids.

Experimental

Materials and methods

Materials. Fmoc-phenylalanine (Fmoc-F) and Fmoc-tyrosine (Fmoc-Y) were purchased from Sigma-Aldrich. 1,2-Dimyristoyl-sn-glycero-3-phosphate (DMPA) phospholipid was purchased from Avanti Lipids and used as received. Solvents were used without further purification and purchased from Aldrich (Germany). Hydrochloric acid 37% was PRS-Codex purchased from Panreac and used as received. The initial 1 mM solutions of Fmoc-F and Fmoc-Y were prepared in dichloromethane. A mixture of chloroform : methanol (3 : 1 in volume) was used for dissolving DMPA at a concentration of 1 mM. The Fmoc-amino acids and the DMPA were co-spread in molar ratio DMPA : Fmoc amino acid 1 : 1. The choice of different solvents for the Fmoc-amino acid derivatives and the phospholipid was motivated to minimize any solubility problems. Considering the high miscibility of the solvents, no phase segregation was expected. Ultrapure water produced by a Millipore Milli-Q unit, and pre-treated by a Millipore reverse osmosis system (>18.2 MΩ cm) was used to prepare the acid solution for subphase. The subphase temperature was 21 °C with pH 2. All experiments were performed on tables with vibration isolation using the antivibration system MOD-2 S (Accurion, Göttingen, Germany) in a large class 100 clean room.

Surface pressure–area (π–A) isotherms. Two different models of Nima troughs (Nima Technology, Coventry, England) were used, both provided with a Wilhelmy type dynamometric system using a strip of filter paper: a NIMA 611D with one moving barrier for the measurement of the reflection spectra, and a NIMA 601, equipped with two symmetrical barriers to record BAM images. The monolayers were compressed at a speed of 0.03 nm^2 per min per molecule. The measurements for the surface pressure–molecular area isotherms were performed at least three times each, obtaining no significant differences.

Brewster angle microscopy (BAM). Images of the film morphology were obtained by Brewster angle microscopy (BAM) with a I-Elli2000 (Accurion GmbH) using a Nd:YAG diode laser with wavelength 532 nm and 50 mW with a lateral resolution of 2 μm. The image processing procedure included a geometrical correction of the image, as well as a filtering operation to reduce interference fringes and noise.

UV-vis reflection spectroscopy. UV-visible reflection spectra at normal incidence as the difference in reflectivity (ΔR) of the film-covered water surface and the bare surface were obtained with a Nanofilm Surface Analysis Spectrometer Ref SPEC^2 (Accurion, Göttingen, Germany).

Computer simulations. All the simulations were performed using HyperChem 7.51.[21] Note that the computational results presented herein offer a qualitative picture of the interactions between DMPA and Fmoc-Y. The simulations were performed *in vacuo* to avoid the large computational cost of simulating the solvent molecules. The molecular structures of the DMPA and Fmoc-Y molecules were optimized by the semiempirical method AM1. After optimization, the DMPA and Fmoc-Y molecules were set with their polar heads pointing to each other. One 5 nanoseconds run of molecular dynamics at a temperature of 500 K was performed to avoid any initial constraint on the configuration of the system. No hydrogen bonds were detected after the run of 2 nanoseconds. Molecular mechanics was applied for finding an optimal configuration, using 300 K and a total run time of 5 nanoseconds. The formation of hydrogen bonds within the C5 molecule was detected during the optimization run.

Conflicts of interest

There are no conflicts to declare.

Acknowledgements

References

1 J. Han, K. Liu, R. Chang, L. Zhao and X. Yan, *Angew. Chem., Int. Ed.*, 2019, **58**, 2000–2004.
2 E. R. Draper, K. L. Morris, M. A. Little, J. Raeburn, C. Colquhoun, E. R. Cross, T. O. McDonald, L. C. Serpell and D. J. Adams, *CrystEngComm*, 2015, **17**, 8047–8057.
3 V. Singh, K. Snigdha, C. Singh, N. Sinha and A. K. Thakur, *Soft Matter*, 2015, **11**, 5353–5364.
4 J. Li, R. Xing, S. Bai and X. Yan, *Soft Matter*, 2019, **15**, 1704–1715.

5 C. Rizzo, R. Arrigo, F. D'Anna, F. Di Blasi, N. T. Dintcheva, G. Lazzara, F. Parisi, S. Riela, G. Spinelli and M. Massaro, *J. Mater. Chem. B*, 2017, **5**, 3217–3229.

6 P. Zhang, Y. Huang, Y. T. Kwon and S. Li, *Mol. Pharm.*, 2015, **12**, 1680–1690.

7 A. Y. Gahane, P. Ranjan, V. Singh, R. K. Sharma, N. Sinha, M. Sharma, R. Chaudhry and A. K. Thakur, *Soft Matter*, 2018, **14**, 2234–2244.

8 P. Xing, X. Chu, S. Li, M. Ma and A. Hao, *ChemPhysChem*, 2014, **15**, 2377–2385.

9 P. G. Argudo, R. Contreras-Montoya, L. Álvarez de Cienfuegos, J. M. Cuerva, M. Cano, D. Alba-Molina, M. T. Martín-Romero, L. Camacho and J. J. Giner-Casares, *Soft Matter*, 2018, **14**, 9343–9350.

10 P. G. Argudo, R. Contreras-Montoya, L. Álvarez de Cienfuegos, M. T. Martín-Romero, L. Camacho and J. J. Giner-Casares, *J. Phys. Chem. B*, 2019, **123**, 3721–3730.

11 R. Vijay and P. L. Polavarapu, *J. Phys. Chem. A*, 2012, **116**, 10759–10769.

12 L. Vugmeyster and D. Ostrovsky, *Chem. Phys. Lett.*, 2017, **673**, 108–112.

13 S. Bera, S. Mondal, Y. Tang, G. Jacoby, E. Arad, T. Guterman, R. Jelinek, R. Beck, G. Wei and E. Gazit, *ACS Nano*, 2019, **13**, 1703–1712.

14 J. J. Giner-Casares, G. Brezesinski and H. Möhwald, *Curr. Opin. Colloid Interface Sci.*, 2014, **19**, 176–182.

15 J. V. N. Ferreira, J. H. G. Lago and L. Caseli, *Chem. Phys. Lett.*, 2019, **717**, 87–90.

16 D. Matyszewska, K. Brzezińska, J. Juhaniewicz and R. Bilewicz, *Colloids Surf., B*, 2015, **134**, 295–303.

17 L. G. Tulli, W. Wang, V. Rullaud, W. R. Lindemann, I. Kuzmenko, D. Vaknin and P. Shahgaldian, *RSC Adv.*, 2016, **6**, 9278–9285.

18 S. Bettini, R. Pagano, V. Borovkov, G. Giancane and L. Valli, *J. Colloid Interface Sci.*, 2019, **533**, 762–770.

19 C. Rubia-Payá, G. De Miguel, M. T. Martín-Romero, J. J. Giner-Casares and L. Camacho, *Adv. Colloid Interface Sci.*, 2015, **225**, 134–145.

20 J. Klug, D. Masone and M. G. Del Pópolo, *RSC Adv.*, 2017, **7**, 30862–30869.

21 *Hyperchem 7.51*, Hypercube, Inc.

22 T. Li, M. Kalloudis, A. Z. Cardoso, D. J. Adams and P. S. Clegg, *Langmuir*, 2014, **30**, 13854–13860.

23 K. Tao, A. Levin, L. Adler-Abramovich and E. Gazit, *Chem. Soc. Rev.*, 2016, **45**, 3935–3953.

24 T. Zhang, S. L. Brantley, D. Verreault, R. Dhankani, S. A. Corcelli and H. C. Allen, *Langmuir*, 2018, **34**, 530–539.

25 A. M. González-Delgado, C. Rubia-Payá, C. Roldán-Carmona, J. J. Giner-Casares, M. Pérez-Morales, E. Muñoz, M. T. Martín-Romero, L. Camacho and G. Brezesinski, *J. Phys. Chem. C*, 2010, **114**, 16685–16695.

26 C. Roldán-Carmona, A. M. González-Delgado, A. Guerrero-Martínez, L. De Cola, J. J. Giner-Casares, M. Pérez-Morales, M. T. Martín-Romero and L. Camacho, *Phys. Chem. Chem. Phys.*, 2011, **13**, 2834–2841.

27 E. C. Griffith, R. J. Perkins, D.-M. Telesford, E. M. Adams, L. Cwiklik, H. C. Allen, M. Roeselová and V. Vaida, *J. Phys. Chem. B*, 2015, **119**, 9038–9048.

28 S. Das, F. Herrmann-Westendorf, F. H. Schacher, E. Täuscher, U. Ritter, B. Dietzek and M. Presselt, *ACS Appl. Mater. Interfaces*, 2016, **8**, 21512–21521.

29 A. C. Alves, C. Nunes, J. Lima and S. Reis, *Colloids Surf., B*, 2017, **160**, 610–618.

30 C. E. McNamee and M. Kappl, *RSC Adv.*, 2016, **6**, 54440–54448.

31 C. Roldán-Carmona, J. J. Giner-Casares, M. Pérez-Morales, M. T. Martín-Romero and L. Camacho, *Adv. Colloid Interface Sci.*, 2012, **173**, 12–22.

32 G. N. Jaroque, P. Sartorelli and L. Caseli, *Biophys. Chem.*, 2019, **246**, 1–7.

33 T. C. F. Santos, L. O. Péres, S. H. Wang, O. N. Oliveira and L. Caseli, *Langmuir*, 2010, **26**, 5869–5875.

34 D. Matyszewska, S. Sek, E. Jabłonowska, B. Pałys, J. Pawlowski, R. Bilewicz, F. Konrad, Y. M. Osornio and E. M. Landau, *Langmuir*, 2014, **30**, 11329–11339.

35 D. Gaspar, M. Lúcio, K. Wagner, G. Brezesinski, S. Rocha, J. L. F. Costa Lima and S. Reis, *Biophys. Chem.*, 2010, **152**, 109–117.

36 C. Pereira-Leite, D. Lopes-de-Campos, P. Fontaine, I. Cuccovia, C. Nunes and S. Reis, *Molecules*, 2019, **24(3)**, 516.

37 A. Colombelli, M. G. Manera, V. Borovkov, G. Giancane, L. Valli and R. Rella, *Sens. Actuators, B*, 2017, **246**, 1039–1048.

38 V. E. Bahamonde-Padilla, J. J. López-Cascales, R. Araya-Maturana, M. Martínez-Cifuentes and B. E. Weiss López, *ChemPhysChem*, 2014, **15**, 1422–1431.

39 A. S. Hansen, L. Du and H. G. Kjaergaard, *J. Phys. Chem. Lett.*, 2014, **5**, 4225–4231.